Spatial frequency mixing by nonlinear charge transport in photorefractive materials

J. Limeres, M. Carrascosa, L. Arizmendi, and F. Agulló-López
Departamento de Física de Materiales, C-IV, Universidad Autónoma de Madrid, E-28049 Madrid, Spain

P. E. Andersen
Optics and Fluid Dynamics Dep., Risø National Laboratory, P.O. Box 49, DK-4000 Roskilde, Denmark
(Received 2 August 2001; published 2 May 2002)

We present a theoretical investigation of the nonlinear phenomenon of spatial frequency mixing in photorefractive materials. In particular, we study the kinetics of the second harmonics and the sum and difference (combinational) gratings when two photorefractive gratings are recorded in the material. The physical origin of the new gratings is extensively discussed. The formalism is applied to investigate multiple recording in $LiNbO_3$ as a material relevant for applications. The influence of the multiple-recording method (either sequential or simultaneous) on the generation of second-order gratings is analyzed. We found remarkable differences in the kinetics of these gratings depending on the multiplexing procedure. Our theoretical predictions are in good agreement with a number of previously reported experimental results.

DOI: 10.1103/PhysRevB.65.195117 PACS number(s): 42.40.Eq, 42.40.Ht, 42.65.Hw

I. INTRODUCTION

The photorefractive (PR) effect[1] consists of a change in the refractive index induced by inhomogeneous illumination of a photoconductor and electro-optic material. In typical PR experiments, a sinusoidal pattern, obtained by the interference of two plane waves, is used. As a result, a sinusoidal diffraction grating, or phase hologram, is recorded in the material. PR media have been proposed for several holographic applications, such as interferometry by real-time holography, optical storage, interconnects, etc.

The physical mechanism of the PR effect involves the redistribution of charge in the material that gives rise to a spatially varying internal electric field. Then this internal electric field leads to the generation of the corresponding refractive index pattern via the electro-optic effect. The former process consists of three steps: (1) optical and/or thermal excitation of carriers from the filled traps, (2) migration of the free carriers in the conduction (or valence) band, and, finally, (3) subsequent recombination of the free carriers at the acceptor sites.

All these three processes—free charge generation, transport, and recombination—take place through a nonlinear mechanism. For single grating recording, a number of phenomena arising from this nonlinearity have been previously investigated (see, for instance, Refs. 2–6 and references therein). However, many situations—e.g., holographic storage or optical interconnects—involve not just one, but several PR holograms (gratings). In such *multigrating* situations, the nonlinear PR response leads to the mutual coupling of the involved gratings and so to new nonlinear PR phenomena. But unlike the single-grating case, less attention has been paid to these nonlinear multigrating effects. Some years ago the so-called *nonlinear grating cross talk* was first observed in the simultaneous recording of two gratings in a BSO crystal.[7] This effect was interpreted as mutual coupling through the nonlinear photoinduced current[8,9] and was further investigated in subsequent works.[10,11] On the other hand, Fries *et al.* reported the generation of a difference grating in sequential recording of two hologram gratings in lithium niobate ($LiNbO_3$).[12] More recently, the sum grating has been observed in the simultaneous recording of two gratings in BSO.[13] Finally, experimental measurements of multiple spatial frequency mixing involving up to fourth-order combinations in the sequential recording of two gratings in $LiNbO_3$ have been published.[14] However, a detailed theoretical analysis of these frequency-mixing problems is still needed. In fact, general theoretical frameworks to describe PR material nonlinearities have been proposed and applied to a variety of parametric processes.[14–16] Unfortunately, they have not been specifically applied to investigate the present problem and only a first simple approach to calculate the kinetics of the frequency-mixing gratings was reported in Ref. 12 for the case of sequential recording.

In this paper we present a general but simple phenomenological approach to account for the dynamics of nonlinear combinational gratings that provides a clear insight into the physics of the involved phenomena. Our approach is an extension of that used in Ref. 12 that includes not only the sum and difference gratings, but also second harmonics. Moreover, the formalism is also applied to investigate the simultaneous recording case that had not considered in that work. Additionally, a more detailed description of the mathematical formalism and discussion of the obtained equations are provided. We will obtain the full kinetics of all second-order gratings (second harmonics and sum and difference holograms). The formalism is specifically applied to photovoltaic PR crystals such as $LiNbO_3$, which is one of the best candidates for PR holographic storage. We will identify the relevant parameters and analyze their influence on the nonlinear processes. A comparison between sequential and simultaneous recording is also provided. Special attention is paid to compare our prediction with recent experimental results.

Our analysis also provides important information for the practical use of PR materials in applications. In particular, results should be relevant for storage and interconnect devices where these higher-order gratings behave as coherent optical noise. On the other hand, the nonlinear mechanisms

provide a new way to record gratings with K vectors that could be difficult to reach directly by two-wave mixing with simple geometrical configurations.[14] Therefore it is useful to provide an analysis of the strength of nonlinear effects, paying attention to the influence of material and experimental parameters on the amplitude of nonlinear gratings.

II. THEORETICAL FORMALISM

We base our study on the usual band transport model for the PR effect[17] whose main features were already mentioned in the Introduction. Specifically, we consider charge transport processes in a photoconductor crystal under illumination with an inhomogeneous light pattern, $I(\mathbf{r})$. Only one kind of optically active trap, with two oxidation states, is assumed. This one-trap model is generally accepted in many PR crystals.

The inhomogeneous illumination induces a redistribution of the space-charge density within the crystal. The corresponding mathematical formulation includes the following rate equations:

$$\frac{\partial N_A(\mathbf{r},t)}{\partial t} = sI(\mathbf{r},t)[N - N_A(\mathbf{r},t)] - \gamma n(\mathbf{r},t) N_A(\mathbf{r},t) \quad (1)$$

and

$$\frac{\partial n(\mathbf{r},t)}{\partial t} = \frac{\partial N_A(\mathbf{r},t)}{\partial t} + \frac{1}{e}\overline{\nabla}\mathbf{j}(\mathbf{r},t), \quad (2)$$

which, respectively, describe the time evolution of N_A, the concentration of acceptors, and n, the free charge density. Here e is the absolute value of the electron charge, N is the total concentration of traps, s is the photoexcitation cross section, and γ is the trapping coefficient. Hence the two terms on the right-hand side of Eq. (1) correspond to the optical excitation of electrons and its subsequent recombination, respectively. In Eq. (2) the additional term involving the gradient of the current density, $\mathbf{j}$, accounts for the migration of carriers. The time derivative $\partial n/\partial t$ in this equation is usually neglected. This is the so-called adiabatic approximation, which relies on the fact that the charge carrier density n reaches equilibrium much faster than the other involved physical variables.

The total current density $\mathbf{j}$ inside the PR crystal is the result of three contributions: (a) the drift term $\mathbf{j}_{\text{drift}}$, (b) the current due to diffusion $\mathbf{j}_{\text{diff}}$, and (c) the photovoltaic contribution $\mathbf{j}_{\text{PV}}$ for materials that exhibit a bulk photovoltaic effect:

$$\mathbf{j} = \mathbf{j}_{\text{drift}} + \mathbf{j}_{\text{diff}} + \mathbf{j}_{\text{PV}} = e\mu n\mathbf{E} + eD\overline{\nabla}n + esIL_{\text{PV}}(N - N_A), \quad (3)$$

where μ is the electronic mobility, D is the diffusion constant and L_{PV} is the photovoltaic length, which characterizes the photovoltaic effect in a given crystal. Finally, the space-charge field $\mathbf{E}$ and the charge density ρ inside the medium are related through the Poisson equation

$$\overline{\nabla}E = \frac{\rho}{\varepsilon\varepsilon_0}, \quad (4)$$

where the charge density ρ is given by $\rho = e(N_A - \langle N_A \rangle)$. As usual, use of brackets $\langle\ \rangle$ denotes the average of the enclosed variable. In this expression the density of free electrons has been neglected in comparison with $(N_A\text{-}\langle N_A \rangle)$ as is usual for low and moderate light intensities.

Equations (1)–(4) describe the space-charge redistribution taking place during PR recording. Our independent variables are the space-charge field $\mathbf{E}$, the free charge carriers density n, and the concentration of acceptors N_A.

To solve these equations one should take into account the continuity of current:

$$\overline{\nabla}j + \frac{\partial \rho}{\partial t} = 0, \quad (5)$$

From Eqs. (3), (4), and (5) one arrives at a very useful equation for the time evolution of the space-charge field $\mathbf{E}$:

$$\frac{\partial \mathbf{E}(\mathbf{r},t)}{\partial t} + \frac{1}{\varepsilon\varepsilon_0}\mathbf{j}(\mathbf{r},t) = \mathbf{j}_0, \quad (6)$$

ε_0 and ε being the vacuum dielectric permitivity and the relative dielectric constant of the medium, respectively, and $\mathbf{j}_0$ is a constant to be determined by the boundary conditions of the problem.

Origin of nonlinear multigrating effects

Let us examine the form of Eqs. (1) and (3). Notice that they contain *four* nonlinear terms, i.e., terms including cross products of spatially modulated quantities. First, Eq. (1) includes the photoexcitation term sIN_A and the trapping term $\gamma n N_A$. In turn, Eq. (3) for the current density contains the products $n \cdot \mathbf{E}$ and $I \cdot N_A$ in the drift and photovoltaic terms, respectively. These nonlinear contributions are actually responsible for the nonlinear coupling of gratings. When several spatial frequencies are involved in the recording process (as is the case of multiplexing of holograms), the cross products couple the different spatial components, thus giving rise to the generation of new combinational gratings whose frequencies are linear combinations of the initial ones. This phenomenon of *spatial frequency mixing*, which has been already observed experimentally (see, e.g., Refs. 7, 12, and 14), is the main concern of this paper.

Let us consider the PR recording of two sinusoidal patterns (phase holograms) which is the simplest case where multigrating effects take place. Let K_1 and K_2 be the spatial frequencies of the two intentionally recorded (primary) gratings. For simplicity, the fringes of both light patterns are taken to be parallel to each other and perpendicular to the X axis (see Fig. 1). Then only variation along the X direction must be considered and our mathematical formulation may be scalar. In order to solve the nonlinear PR equations we express the dynamic variables as a one-dimensional Fourier expansion in terms of the two fundamental frequencies and including nonlinear combinations of them:

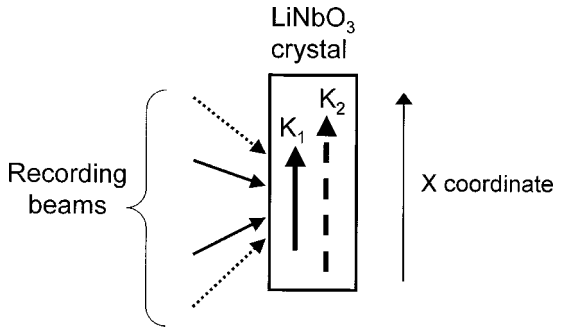

FIG. 1. Schematics of the considered experimental configuration.

$$E(x,t)=\sum_{n,m} E_{nK_1+mK_2}(t)e^{i(nK_1+mK_2)\cdot x}+\text{c.c.}, \qquad (7a)$$

$$N_A(x,t)-N_A^0=\sum_{n} N_{nK_1+mK_2}(t)e^{i(nK_1+mK_2)\cdot x}+\text{c.c.}, \qquad (7b)$$

$$n(x,t)-\langle n(x,t)\rangle=n(x,t)-n_0 = \sum_{n} n_{nK_1+mK_2}(t)e^{i(nK_1+mK_2)\cdot x}+\text{c.c.} \qquad (7c)$$

In order to keep the degree of complexity of the calculations below a reasonable level, we will assume that the Fourier terms higher than second order are negligible. That is, we will only keep in our formulation the two fundamental frequencies K_1 and K_2 and their second harmonics $2K_1$ and $2K_2$, plus the two second-order combinational frequencies $K_+\equiv K_1+K_2$ (*sum* frequency) and $K_-\equiv K_1-K_2$ (*difference* frequency). This assumption is in accordance with experimental data reported in Ref. 12 in which second-order grating amplitudes are much greater than higher-order components. After substitution of expressions (7) into the set of equations (1), (2), (3), and (6), a number of coupled relations would be obtained, which would allow one to calculate the kinetics of the different fundamental and second-order gratings. In the next section the formalism will be specifically applied to multiple recording in $LiNbO_3$, one of the most useful PR media for storage applications. From the theoretical point of view, the situation in $LiNbO_3$ permits a further simplification because the dominant nonlinear term is nE and the other ones can be neglected (see below). Besides, this material has been used in several previous experiments on the behavior of combinational gratings,[12,14] whose results may be compared with the theoretical predictions.

III. RESULTS: APPLICATION TO $LiNbO_3$

Usually, in Fe-doped $LiNbO_3$ the donor and acceptor concentrations are high enough so that after recording the contrast of the trap gratings is low. Then the second-order modulated terms originating from γnN_A and sIN_A are negligible in comparison with the second-order terms arising from the drift term $e\mu nE$. Estimates of these modulated terms using experimental parameters of $LiNbO_3$:Fe samples are presented in Ref. 14, confirming our assumption. Hence, in expression (7b), we only keep the nonmodulated component of N_A, whereas the other expansions for n and E are unchanged. This simplifies much of the mathematical treatment as we will see in the next subsections.

Two main procedures are typically used to record a certain number of holograms in a PR material: sequential and simultaneous recording. In the former, the crystal is consecutively exposed to the two sinusoidal patterns, whereas in the latter the two gratings are simultaneously recorded in the medium. These two methods imply different conditions for the generation of second-order gratings, so we will analyze them separately in Secs. III A and III B, respectively. We will discuss in detail the kinetics of the different gratings for typical $LiNbO_3$:Fe crystals. The results will be illustrated with some figures for which we will take the following parameters: $E_{PV}=100$ kV/cm and $K_1=7\ \mu\text{m}^{-1}$ and $K_2=10\ \mu\text{m}^{-1}$. Anyhow, it should be noted that for these typical values of the photovoltaic field and grating K vectors one has $E_D \ll E_{PV}$, and the curves will be nearly independent of the values of K_1 and K_2.

A. Sequential recording

Sequential recording is the usual method to record multiple holograms for storage applications. In this case the crystal is consecutively illuminated by a number of sinusoidal patterns:

$$I_j(x)=\frac{I_0}{2}(1+m_j e^{iK_j\cdot x})+\text{c.c.}, \qquad (8)$$

where $j=1,2,\ldots$. Usually, it is desirable that all the stored holograms have the same diffraction efficiency, and so the exposure times of holograms have to be progressively reduced following a determined time schedule.[18]

As previously mentioned, our analysis will consider the sequential recording of two holograms G_1 and G_2 with grating K vectors K_1 and K_2. After writing a first PR grating (grating G_1) in the medium, the physical variables (n,N_A,E) become spatially modulated with fundamental frequency K_1. During recording of the second grating (grating G_2), the light pattern is again characterized by one single spatial frequency K_2. However, now the material is already imprinted with the previous fundamental frequency K_1, so that combinations of gratings may appear as discussed above. Note that in principle a second-harmonic grating $2K_1$ would be also present in the material. Let $E^0_{K_1}$ and $E^0_{2K_1}$ be the fundamental- and second-harmonic initial amplitudes of these gratings.

To obtain the dynamical equations during the second recording process we put the corresponding intensity pattern (8) (with $j=2$) into expression (3) for the current density; then, we introduce the latter into the time evolution equation (6). Finally, we bring together the terms corresponding to each spatial component of the space-charge field. The procedure is similar to that followed in Ref. 12, although in our formalism second-harmonic gratings are not neglected. This

is in accordance with experimental results,[14] which show that second-harmonic amplitudes are comparable to those of combinational gratings. The obtained set of coupled dynamical equations is written as

$$\frac{dE_{K_1}}{dt}+\frac{1}{\tau}E_{K_1}=-\frac{1}{\tau}(m_2^*E_{K_+}+m_2E_{K_-}), \tag{9a}$$

$$\frac{dE_{2K_1}}{dt}+\frac{1}{\tau}E_{2K_1}=0, \tag{9b}$$

$$\frac{dE_{K_2}}{dt}+\frac{1}{\tau}E_{K_2}=-\frac{1}{\tau}(m_2^*E_{2K_2}+m_2E_{\mathrm{eff}}^{K_2}), \tag{9c}$$

$$\frac{dE_{2K_2}}{dt}+\frac{1}{\tau}E_{2K_2}=-\frac{1}{\tau}m_2E_{K_2}, \tag{9d}$$

$$\frac{dE_{K_+}}{dt}+\frac{1}{\tau}E_{K_+}=-\frac{1}{\tau}m_2E_{K_1}, \tag{9e}$$

$$\frac{dE_{K_-}}{dt}+\frac{1}{\tau}E_{K_-}=-\frac{1}{\tau}m_2^*E_{K_1}, \tag{9f}$$

where $\tau=\varepsilon\varepsilon_0/e\mu_e n_0$ is the dielectric relaxation time and $E_{\mathrm{eff}}^{K_2}=iE_D^{K_2}+E_{\mathrm{PV}}$, $E_D^{K_2}=(K_BT/e)K_2$ and $E_{\mathrm{PV}}=(L_{\mathrm{PV}}\gamma/\mu)N_A$ being the so-called diffusion and photovoltaic fields (see, for instance, Ref. 19). In the expression of the diffusion field, K_B is obviously the Boltzman constant and T the absolute temperature. Because the formalism is derived for the space-charge field components, we will use the term grating amplitudes in order to refer to the space-charge field grating amplitudes in the rest of the paper.

These equations must be solved with the following initial conditions:

$$E_{K_1}(t=0)=E_{K_1}^0,\quad E_{2K_1}(t=0)=\overset{0}{}_{2K_1},$$

$$E_{K_2}(t=0)=E_{2K_2}(t=0)=E_{K_+}(t=0)=E_{K_-}(t=0)=0. \tag{10}$$

First of all, let us briefly consider the structure of set (9). Equations (9a) and (9b) describe the erasure of the fundamental and second harmonic of the first recorded grating, whereas Eqs. (9c) and (9d) describe the buildup of the fundamental and second harmonic components of the second recorded hologram. These latter equations (9c) and (9d) are not coupled with the other equations, so that gratings E_{K_2} and E_{2K_2} develop independently just as if they were alone. In other words, they are not affected by nonlinear interaction effects. Conversely, the spatial components K_+, K_- [Eqs. (9e) and (9f)] and K_1 undergo nonlinear feedback through a number of coupling terms placed on the right-hand side of the corresponding equations. These terms are responsible for the generation of mixing gratings as well as for modifications in the erasure behavior of grating G_1. Finally, the second-harmonic grating of hologram G_1 [Eq. (9b)] is erased without any coupling to other components. Hence it follows a typical optical erasure under homogeneous illumination. Let us analyze in detail the kinetics of the different gratings:

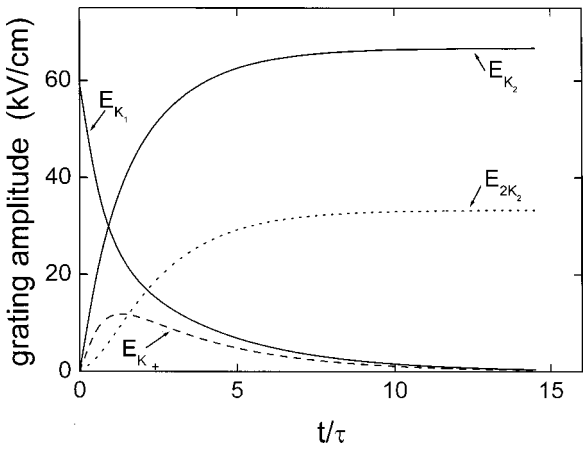

FIG. 2. Time evolution of the grating amplitudes in sequential recording ($m_1=m_2=1$).

1. Combinational gratings

The kinetics of these gratings is controlled by Eqs. (9e) and (9f) coupled to Eq. (9a). Both equations are formally identical, so both gratings have the same time evolution. For instance, let us look at the equation for K_+: the driving term of this grating is $(m_2/\tau)E_{K_1}$. Then the generation of combinational gratings is determined by the presence in the material of grating G_1 and by the illumination with an intensity pattern with modulation m_2. Note that, unexpectedly, the space-charge field E_{K_2} does not play any role. One can easily solve the set of three coupled equations for K_1, K_+, and K_-. The analytical solution for K_+ is written as

$$E_{K_+}(t)=e^{i\phi}E_{K_1}^0(e^{-(1-|m_2|/\sqrt{2})t/\tau}-e^{-(1+|m_2|/\sqrt{2})t/\tau}), \tag{11}$$

where $e^{i\phi}$ is a phase factor that accounts for the phase of the light pattern.

Formula (11) contains the difference of two decaying exponential terms with different characteristic time constants, both depending on m_2. In turn, the preexponential factor and so the amplitude of the sum component depend linearly with the initial amplitude of the fundamental grating K_1. The time evolution of the sum grating has been plotted in Fig. 2 (solid line) for the maximum value of the modulation $m_2=1$ together with curves corresponding to the evolution of both fundamental gratings (dashed line). The time scale is normalized to the dielectric relaxation time τ. The initial growth of E_{K_+} stops at a point that approximately coincides with the crossing point of both fundamental amplitudes. At this point the amplitude E_{K_+} approaches a significant value around 40% of the fundamental gratings. Note that it is at this point when the recording of the second grating K_2 should be stopped in the usual sequential recording experiments because there the two fundamental amplitudes are approximately equal. This occurs at a time

$$t_{\max}=\frac{\tau}{|m_2|\sqrt{2}}\ln\left|\frac{1+|m_2|/\sqrt{2}}{1-|m_2|/\sqrt{2}}\right|. \tag{12}$$

The corresponding maximum amplitude for the sum grating is

$$E_{K_+}^{\max}=\frac{1}{\sqrt{2}}e^{i\phi}E_{K_1}^0\frac{1}{\sqrt{1-|m_2|^2/2}}\left|\frac{1+|m_2|/\sqrt{2}}{1-|m_2|/\sqrt{2}}\right|^{-1/|m_2|/\sqrt{2}}. \tag{13}$$

Then the maximum value of E_{K_+} is linear with $E_{K_1}^0$ as was found in experimental results reported in Refs. 12 and 14. The dependence on m_2 seems to be much more complicated, but it results in being almost linear within a very high degree of accuracy. This linear dependence on m_2 is evident in the short-writing-time limit expression that corresponds to the initial part of the solid curve in Fig. 3, which is written as

$$E_{K_+}=\frac{|m_2|}{\tau}e^{i\phi}E_{K_1}^0 t. \tag{14}$$

This kind of dependence has been also experimentally observed.[14]

2. Second-harmonic gratings

It is also worthwhile to compare the time behavior of both kinds of second-order gratings, i.e., second-harmonic and combinational gratings. The analytic solution for amplitude E_{2K_2} is given by

$$E_{2K_2}(t)=\frac{m_2^2/2}{1-|m_2|/2}E_{\text{eff}}^{K_2}\times\left[1+\left(\frac{1}{|m_2|}-\frac{1}{2}\right)\exp[-(1+|m_2|/2)t/\tau]-\left(\frac{1}{|m_2|}+\frac{1}{2}\right)\exp[-(1-|m_2|/2)t/\tau]\right]. \tag{15}$$

This kinetics E_{2K_2} was also illustrated in Fig. 2 (dashed line) where it may be compared with the time evolution of the sum grating. This latter grating exhibits a nonzero initial slope and, at short times, is generated much faster than the second harmonic. This is due to the distinct source terms for the two gratings which are affected by E_{K_1} in the case of the combinational grating and by E_{K_2} in that of the second harmonic. In particular, at the time $t_{\max}$ the amplitude of the second harmonic is lower than that of the sum and difference gratings. The situation changes at longer times where the combinational gratings decrease to zero due to the decay of K_1, whereas the second-harmonic gratings still progress to a higher steady level as K_2 keeps increasing. This different behavior is also in accordance with previous experimental data.[14]

3. Effects on the fundamental gratings

As previously mentioned, the kinetics of the second fundamental grating [Eq. (9b)] is not influenced by nonlinear grating interactions. However, the decay of the first fundamental grating [Eq. (9a)] is slowed down by the nonlinear feedback coming from the cross products $m_2^* E_{K_+}+m_2 E_{K_-}$. In Fig. 3, $E_{K_1}(t)$ has been plotted together with the evolution of $E_{K_2}(t)$. For comparison, the simple single-grating optical erasure (dashed line) is also plotted. Note that the time at which both fundamental gratings are equal is smaller and the corresponding amplitudes slightly larger ($\sim$5%) than in the linear case. Hence these predictions might affect the optimum time schedule for sequential recording of multiple holograms in $LiNbO_3$.

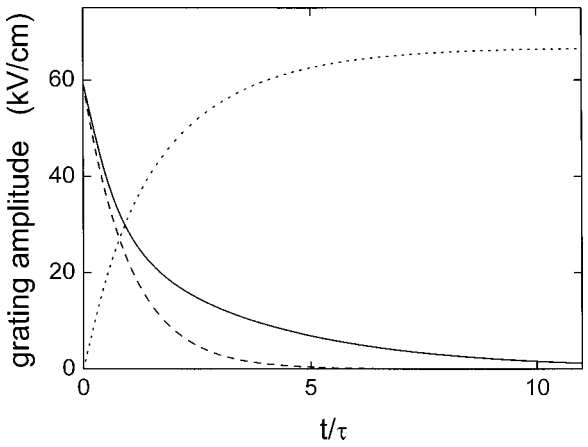

FIG. 3. Time evolution of grating amplitudes E_{K_1} (solid line) and E_{K_2} (dotted line) during sequential recording. Dashed line: single-grating optical erasure kinetics of the grating K_1 ($m_1=m_2=1$).

B. Simultaneous recording

Let us consider now the generation of second-order gratings during simultaneous recording, i.e., when the two light patterns with spatial frequencies K_1 and K_2 illuminate at the same time the PR crystal. To avoid the buildup of undesirable gratings the light beams used to record each grating must be incoherent with those generating the other one. This is the situation for wavelength multiplexing where the incoherence requirement is inherent to the experimental technique. In angular multiplexing, configurations keeping these mutual incoherence conditions have been used for the implementation of optical light interconnects[20] or optical processing operations such as matrix multiplication.[21]

Let us consider for simplicity a recording light pattern consisting of two parallel sinusoidal patterns with frequencies K_1 and K_2:

$$I(x)=\frac{I_0}{2}(1+m_1e^{iK_1\cdot x}+m_2e^{iK_2\cdot x})+\text{c.c.} \tag{16}$$

In this case the gratings are generated at the same time, all of them starting from zero initial conditions. Analogously to Sec. III A, we obtain the following set of equations describing the kinetics of the grating amplitudes:

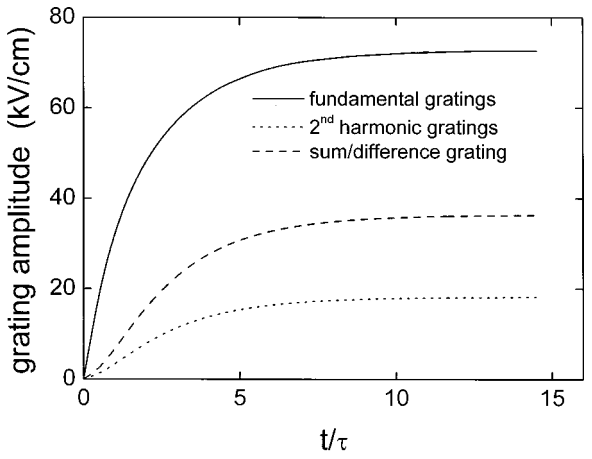

FIG. 4. Time evolution of the grating amplitudes during simultaneous recording ($m_1=m_2=0.5$).

$$\frac{dE_{K_1}}{dt}+\frac{1}{\tau}E_{K_1}=-\frac{1}{\tau}(m_1^*E_{2K_1}+m_2^*E_{K_+}+m_2E_{K_+}^*+m_1E_{\text{eff}}^{K_1}), \tag{17a}$$

$$\frac{dE_{K_2}}{dt}+\frac{1}{\tau}E_{K_2}=-\frac{1}{\tau}(m_2^*E_{2K_2}+m_1^*E_{K_+}+m_1E_{K_-}+m_2E_{\text{eff}}^{K_2}), \tag{17b}$$

$$\frac{dE_{2K_1}}{dt}+\frac{1}{\tau}E_{2K_1}=-\frac{1}{\tau}m_1E_{K_1}, \tag{17c}$$

$$\frac{dE_{2K_2}}{dt}+\frac{1}{\tau}E_{2K_2}=-\frac{1}{\tau}m_2E_{K_2}, \tag{17d}$$

$$\frac{dE_{K_+}}{dt}+\frac{1}{\tau}E_{K_+}=-\frac{1}{\tau}(m_1E_{K_2}+m_2E_{K_1}), \tag{17e}$$

$$\frac{dE_{K_-}}{dt}+\frac{1}{\tau}E_{K_-}=\frac{1}{\tau}(m_1^*E_{K_2}+m_2E_{K_1}^*). \tag{17f}$$

Compared with Eqs. (9), these equations show a number of differential features. First of all, the equations for G_1 and G_2—Eqs. (17a) and (17b)—are formally identical, as they correspond to an equal physical situation for both gratings. Second, the dynamics of both fundamental gratings is affected by nonlinear terms associated with all second-harmonic gratings. Finally, the time evolution of all second-order gratings (either harmonics or combinational) is coupled via the fundamental gratings.

1. Combinational and second-harmonic gratings

Let us further analyze the dynamics of the second-order gratings. The numerical solution of Eqs. (17) is presented as curves plotted in Fig. 4 for maximum light modulation depths that in simultaneous recording correspond to $m_1=m_2=0.5$. Let us consider now carefully the behavior of each grating.

As in sequential recording, the amplitudes of both sum and difference gratings follow identical kinetic behaviors, but in this case, the combinational components are not transient because now none of the fundamental gratings is being erased during the recording process. In the steady state the amplitudes E_{K_+} and E_{K_-} are 50% of the fundamental ones, 10% higher than in sequential recording. Finally, at variance with sequential recording the maximum value of combinational gratings is substantially greater than that of second harmonics. Although there are no available experimental data for simultaneous recording in $LiNbO_3$, this latter result is in qualitative accordance with some observations in BSO,[13] in which the sum grating was substantially greater than the second harmonic.

Equations (17) may be analytically solved, but the solution is too complicated to be useful. However, it is possible to obtain very simple expressions for the second-order gratings under a quite drastical approach. The procedure is as follows: the linear solutions of the fundamental gratings—i.e., the ones obtained by neglecting all second-order terms in Eqs. (17a) and (17b)—are introduced into Eqs. (17e) and (17f). Then these latter equations are immediately solved, leading to approximate analytical expressions for all second-order gratings. This approximation is strictly valid as long as both second-harmonic and spatial-mixing gratings are much smaller than the fundamental gratings. The approximated expressions for the sum and difference gratings are written, respectively,

$$E_{K_+}(t)=m_1m_2(E_{\text{eff}}^{K_2}+E_{\text{eff}}^{K_1})\left[1-\left(1+\frac{t}{\tau}\right)\exp(-t/\tau)\right], \tag{18a}$$

$$E_{K_-}(t)=m_1^*m_2(E_{\text{eff}}^{K_2}+E_{\text{eff}}^{K_1^*})\left[1-\left(1+\frac{t}{\tau}\right)\exp(-t/\tau)\right], \tag{18b}$$

and for the second harmonics,

$$E_{2K_1}(t)=m_1^2E_{\text{eff}}^{K_1}\left[1-\left(1+\frac{1}{\tau}\right)\exp(-t/\tau)\right], \tag{19a}$$

$$E_{2K_2}(t)=m_2^2E_{\text{eff}}^{K_2}\left[1-\left(1+\frac{t}{\tau}\right)\exp(-t/\tau)\right]. \tag{19b}$$

All second-order components exhibit the same time dependence, although for combinational gratings there are two nonlinear contributions, whereas for the second harmonics there exists only one. This is the reason for the higher steady level of combinational gratings. On the other hand, the strength of nonlinear gratings is controlled by the square of the light modulation depths. To evaluate the accuracy of approximate solutions we compared them with the exact solutions in Fig. 5. There the sum and difference kinetics are plotted for maximum ($m_1=m_2=0.5$) and intermediate ($m_1=m_2=0.3$) light modulations. Note that for the latter modulations the deviations between the approximate and exact

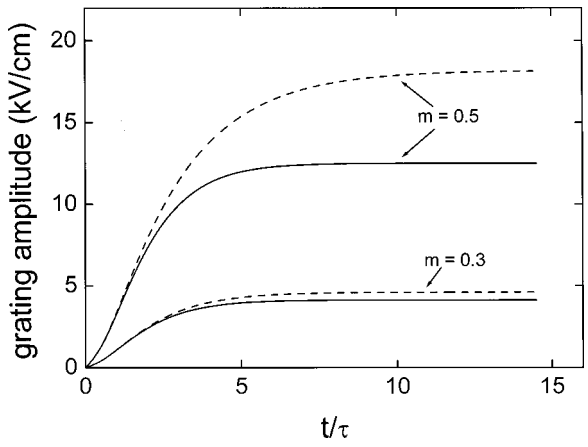

FIG. 5. Time evolution of the combinational grating amplitudes during simultaneous recording for $m=0.5$ and 0.3. Solid line: exact numerical solution. Dashed line: approximate analytical solution (see text).

curves are very small. For maximum modulations the two curves are very close at short times, but differ significantly ($\sim$30%) in the steady state.

2. Fundamental gratings and nonlinear cross talk

It is also interesting to evaluate the influence of nonlinear coupling on fundamental grating amplitudes. We present in Fig. 6(a) the exact multigrating solution for the fundamental amplitudes E_{K_1} and E_{K_2} (solid lines) together with the single grating approximation (i.e., neglecting combinational gratings) for the same modulations. Notice that, unlike the case of sequential recording, E_{K_2} as well as E_{K_1} are significantly affected by nonlinear interactions. This effect, called *nonlinear cross talk*, has been previously investigated though in different situations and materials.[7,22] Notice that nonlinear feedback leads to an enhancement of 30% of the fundamental grating amplitudes. A similar amplification effect has been experimentally observed in simultaneous recordings in an analogous configuration but in barium titanate crystal.[22]

It is worthwhile to point out that the final amplitude of second harmonics is also markedly influenced by multigrating interactions. This is shown in Fig. 6(b) where the multigrating solution for the second harmonics (solid line) is plotted together with the single-grating case (dashed line). It is clearly seen that, as in the case of fundamental components, nonlinear cross talk leads to an enhancement of the second-harmonic amplitudes.

IV. DISCUSSION AND CONCLUSIONS

Spatial frequency mixing in photovoltaic materials like $LiNbO_3$ has been theoretically investigated. This phenomenon takes place in multigrating experiments due to the nonlinear mechanisms for charge transport in PR materials.

For our analysis we use a simple approach that includes the fundamental intentionally recorded gratings together with all terms up to second order. Within this mathematical framework the time-dependent solutions for the amplitudes of all gratings have been obtained.

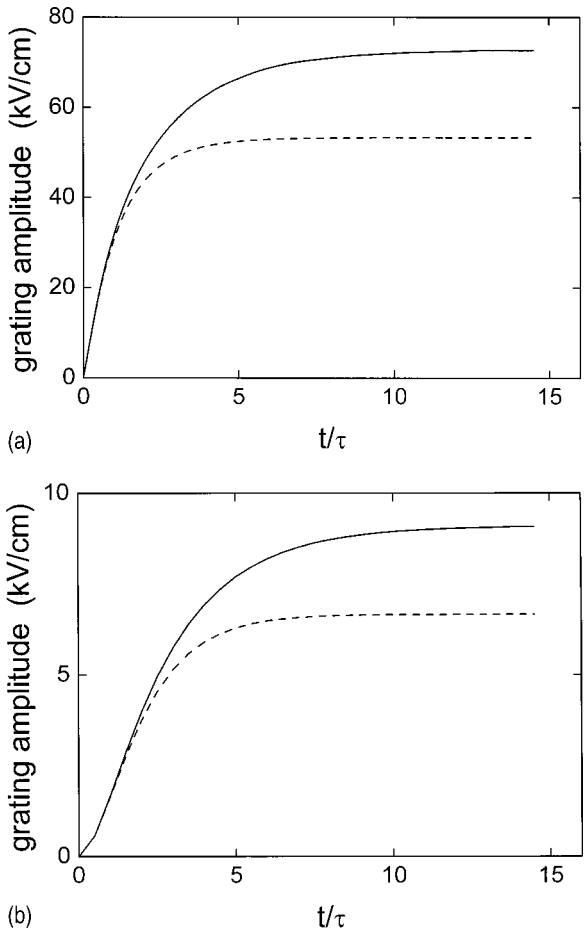

FIG. 6. (a) Time evolution of the fundamental grating amplitudes. (b) Time evolution of the second-harmonic amplitudes. Solid line: simultaneous recording kinetics. Dashed line: single-grating recording ($m_1=m_2=0.5$).

We have considered the two main typical methods for multiple hologram recording: i.e., sequential and simultaneous operations. For both methods, the combinational grating amplitudes reach very significant relative values with regard to the fundamental ones—40% and 50% for sequential and simultaneous operations, respectively—and they are substantially greater than second harmonics.

For simultaneous recording, as may be expected from analogy with nonlinear effects in single-grating recording, the key parameters that control the generation of combinational gratings are the modulations of light patterns. However, for sequential operation, the controlling parameters are the amplitude of the first grating and the modulation of the second light pattern, whereas the contrast of the first light pattern is not relevant. On the other hand, we have obtained that the relative amplitude of combinational gratings does not depend on material parameters and grating K vectors.

There are still a number of other features that are different depending on the multiplexing method.

(a) Regarding the kinetics of combinational gratings, the initial slope is larger for sequential recording, whereas the final amplitude is greater (a factor of $\sim$1.7) in simultaneous recording. This different behavior has been illustrated in Fig.

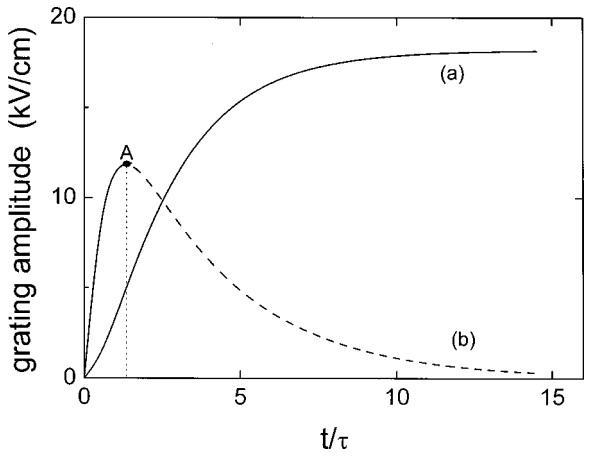

FIG. 7. Time evolution of the combinational gratings in simultaneous [curve (a)] and sequential [curve (b)] recording. In the case of sequential recording, the solid-line curve ends at point *A* (when the amplitudes of the fundamental gratings are equal), the rest of the kinetics being given as the dashed line (see text).

7. Notice that the sequential-recording kinetics [curve (a)] has been drawn as a solid line until the time for which both fundamental gratings have the same amplitude. At this time the recording of the grating K_2 is stopped in typical sequential multiplexing experiments.

(b) The existence of nonlinear interactions only shows a very small effect (less than 5%) on the fundamental amplitudes of sequentially multiplexed holograms (see Fig. 3). On the other hand, in simultaneous recording grating cross talk effects are important and markedly enhance the grating amplitudes (30%).

(c) In simultaneous recording the behaviors of all second-order gratings are coupled via the fundamental gratings, whereas in sequential recording (and always within our degree of approximation) second harmonics and combinational gratings behave independently.

It is worthwhile to remark that, as mentioned, our theoretical results are in good agreement with available experimental data for sequential recording in $LiNbO_3$. Moreover, our approach could be fully applied to other PR media as long as the condition of low trap modulation is fulfilled. However, for materials such as BSO and BTO whose acceptor concentration is usually low ($\sim 10^{16}$ cm^{-3}), it is necessary to apply the general framework preserving all nonlinear terms. Nevertheless, qualitative agreement with some experimental results of simultaneous recording in BSO and $BaTiO_3$ have been also obtained.

ACKNOWLEDGMENTS

We want to acknowledge financial support from the Spanish Ministerio de Educación y Cultura (Grants Nos. PB97-0008 and PB98-0056) and Comunidad de Madrid (Grant No. 07T/0043/2000).

[1] L. Solymar, D. J. Webb, and A. Grunet-Jepsen, *The Physics and Applications of Photorefractive Materials* (Oxford University Press, Oxford, 1997).
[2] T. J. Hall, R. Jaura, L. M. Connors, and P. D. Foote, Prog. Quantum Electron. **10**, 77 (1985).
[3] E. Serrano, V. Lopez, M. Carrascosa, and F. Agulló-López, J. Opt. Soc. Am. B **11**, 670 (1994); IEEE J. Quantum Electron. **30**, 875 (1994).
[4] S. Mallick, B. Imbert, H. Ducollet, J. P. Herriau, and J. P. Huignard, J. Appl. Phys. **63**, 5660 (1988).
[5] G. F. Calvo, B. Sturman, F. Agulló-López, and M. Carrascosa, Phys. Rev. Lett. **84**, 3839 (2000).
[6] Zh. Zhou, Xd. Sun, Y. Li, Y. Y. Jiang, H. Zhao, K. Xu, and Q. Y. Wan, J. Opt. Soc. Am. B **13**, 2580 (1996).
[7] P. E. Andersen, P. M. Petersen, and P. Buchhave, Appl. Phys. Lett. **65**, 271 (1994).
[8] P. E. Andersen, P. Buchhave, P. M. Petersen, and M. V. Vasnetsov, J. Opt. Soc. Am. B **12**, 1422 (1995).
[9] H. C. Pedersen, P. E. Andersen, P. M. Petersen, and Per M. Johansen, J. Opt. Soc. Am. B **13**, 2569 (1996).
[10] P. E. Andersen, P. M. Petersen, and P. Buchhave, J. Opt. Soc. Am. B **12**, 2453 (1995).
[11] J. Limeres, M. Carrascosa, F. Agulló-López, P. E. Andersen, and P. M. Petersen, J. Opt. Soc. Am. B **16**, 414 (1999); J. Limeres, M. Carrascosa, P. E. Andersen, and P. M. Petersen, OSA Trends Opt. Photonics Ser. **27**, 394 (1999).
[12] S. Fries, S. Bauschulte, E. Krätzig, K. Ringhofer, and Y. Yacobi, Opt. Commun. **84**, 251 (1991).
[13] P. E. Andersen and P. M. Petersen, J. Opt. Soc. Am. B **15**, 2032 (1998).
[14] E. M. de Miguel-Sanz, J. Limeres, L. Arizmendi, and M. Carrascosa, J. Opt. Soc. Am. B **16**, 414 (1999).
[15] B. I. Sturman, M. Mann, J. Otten, and K. Ringhofer, J. Opt. Soc. Am. B **10**, 1919 (1993).
[16] H. C. Pedersen and P. Johansen, J. Opt. Soc. Am. B **12**, 1065 (1995); Phys. Rev. Lett. **77**, 3106 (1996).
[17] N. V. Kukhtarev, V. B. Markov, S. G. Odulov, M. S. Soskin, and V. L. Vinetskii, Ferroelectrics **22**, 949 (1979).
[18] E. S. Maniloff and K. M. Johnson, J. Appl. Phys. **70**, 4702 (1991).
[19] M. Aguilar, M. Carrascosa, F. Agulló-López, and E. Serrano, J. Opt. Soc. Am. B **14**, 110 (1997).
[20] P. Astana, G. P. Nordin, A. R. Tanguay, Jr., and B. Keith Jenkins, Appl. Opt. **32**, 1441 (1993).
[21] C. Gu, S. Campbell, and P. Yeh, Opt. Lett. **18**, 146 (1993).
[22] J. Limeres, M. Carrascosa, P. M. Petersen, and P. E. Andersen, J. Appl. Phys. **88**, 5527 (2000).